Chemical Engineering Journal 465 (2023) 142770

Contents lists available at ScienceDirect

Chemical Engineering Journal

journal homepage: www.elsevier.com/locate/cej

Cytochrome P450-mediated co-metabolism of fluoroquinolones by *Haematococcus lacustris* for simultaneously promoting astaxanthin and lipid accumulation

Xiang Wang [a,*], Zhong-Hong Zhang [a], Kuan-Kuan Yuan [a], Hui-Ying Xu [a], Guo-Hui He [a], Libin Yang [b], Joseph Buhagiar [d], Wei-Dong Yang [a], Yalei Zhang [b,*], Carol Sze Ki Lin [c], Hong-Ye Li [a,*]

[a] *Key Laboratory of Eutrophication and Red Tide Prevention of Guangdong Higher Education Institutes, College of Life Science and Technology, Jinan University, Guangzhou 510632, China*
[b] *State Key Laboratory of Pollution Control and Resources Reuse, College of Environmental Science and Engineering, Tongji University, Shanghai 200092, China*
[c] *School of Energy and Environment, City University of Hong Kong, Tat Chee Avenue, Kowloon, Hong Kong, China*
[d] *Department of Biology, University of Malta, Msida, Malta*

ARTICLE INFO

Keywords:
Haematococcus lacustris
Glycerol-mediated co-metabolism
Fluoroquinolone biodegradation
Astaxanthin
Cytochrome P450

ABSTRACT

Microalgae-based antibiotic removal treatment has attracted attention because of its low carbon and sustainable advantages. The microalgal co-metabolism system with a suitable carbon source leads to enhanced performance of pollutant removal. However, currently, limited knowledge is available for the removal of fluoroquinolone using a microalgae-mediated co-metabolism system. In this study, we first investigated that the biotic processes by alga *Haematococcus lacustris* in the co-metabolism system by adding glycerol would be the main contributors responsible for the removal of 10 mg/L ofloxacin (OFL) with the efficiency of 79.73% and the removal of 10 mg/L enrofloxacin (ENR) with the efficiency of 54.10%, respectively. Furthermore, we found that pyruvate from glycerol was converted into substrates and precursors, thereby resulting in the significant accumulations of microalgal astaxanthin and lipid. The astaxanthin content of *H. lacustris* was achieved at 4.81% and 4.69% treated with OFL and ENR in the presence of glycerol, with 16.04% and 14.55% of lipid content, respectively. The proposed metabolites and pathways were identified to plausibly explain the biodegradation of fluoroquinolone by *H. lacustris*. The molecular analyses demonstrated that cytochrome P450 (CYP450) enzymes are responsible for the biodegradation of fluoroquinolone, and it was further verified that fluoroquinolones might insert into CYP450 to finally form an efficient and tight binding conformation by molecular dynamic simulation. These findings provide a microalgae-based route for feasible and sustainable biodegradation of antibiotics using a co-metabolism strategy comprising glycerol as a carbon source, with the synergistic accumulation of valuable products.

1. Introduction

Numerous types of antibiotics were developed and widely used as therapeutic agents for the treatment and prevention of bacterial infections that occurred in both humans and animals. Global antibiotic consumption and usage have become more demanding over the past decades, which results in the rising concentrations of antibiotic residues released through sewage and waste discarded into the aquatic and terrestrial environments. Among the various antibiotics, fluoroquinolones (e.g., ofloxacin, OFL, and enrofloxacin, ENR), as broad-spectrum antibacterial and the third largest sales of antibiotics, attract considerable attention due to their widespread applications in hospital, household, animal husbandry and aquaculture. It is reported that fluoroquinolone sales in food animals and clinical outpatients increased at a high level in the United States, although the United States Food and Drug Administration updated the boxed warning on fluoroquinolones in 2016 [1–3]. In China, fluoroquinolones were considered emerging contaminants distributed in marine, municipal wastewater,

* Corresponding authors.
E-mail addresses: xiangwang@jnu.edu.cn (X. Wang), zhangyalei@tongji.edu.cn (Y. Zhang), thyli@jnu.edu.cn (H.-Y. Li).

https://doi.org/10.1016/j.cej.2023.142770
Received 25 January 2023; Received in revised form 8 March 2023; Accepted 1 April 2023
Available online 3 April 2023

landfills, etc [4–6]. Relevant surveys demonstrated that up to 70% of OFL and ENR by incomplete metabolism are directly excreted into surrounding areas, with the concentrations ranging from ng/L to mg/L levels in the aqueous environment [7,8]. On account of the acute and chronic toxicity of OFL and ENR to aquatic organisms even at low concentrations, they can finally exact a heavy toll on the aquatic ecosystem and even human health issues [9]. Besides, more seriously, trace levels of antibiotics already induce the evolution and development of antibiotic-resistant bacteria and antibiotic-resistance genes, thereby posing potential environmental risks [10]. For instance, fluoroquinolones showed a significant upregulation of antibiotic-resistance genes correlated with *Rhodococcus*, which might increase the risk of disease transmission and the probability of drug-resistant pathogens [11]. The overconsumption of antibiotics accelerates the increasing concentrations of antibiotics in the global environment, resulting in serious threats on the ecosystem and even public health issues [9]. As such, it is of significant importance to prospect sustainable and efficient removal techniques of fluoroquinolone antibiotics from the aquatic environment.

Conventional wastewater treatment plants (WWTPs) are considered to remove pollutants from the sewage to generate clean water compliant with effluent discharge standards; however, they are not designed for effective and adequate removal of antibiotics, and therefore, the remaining antibiotics residual from the WWTP effluent can be also considered as a primary source released into the aquatic environment [12,13]. Despite physical and chemical treatments that have been developed for the high-efficient removal of antibiotics, the specific limitations and drawbacks (e.g., the undesirable byproducts and expensive cost) restrain their realistic application [14]. Alternatively, biological processes could be a sustainable strategy to potentially enhance the dissipation of antibiotics and even completely mineralize antibiotics [15]. Recently, microalgae-based biological treatment has attracted much attention due to the inexpensive and effective removal of antibiotics accompanied by the accumulation of valuable products in conjunction with the principles of 'waste-to-wealth' [13,16,17]. Moreover, it is advantageous that microalgae-based treatment is low-carbon and renewable, which improves carbon footprint through carbon capturing and utilization technologies [17]. It is worthwhile noting that the removal efficiency of antibiotics is highly based on the species of microalgae [18]. *Haematococcus lacustris* (previously named *Haematococcus pluvialis*), as a unicellular green alga, is capable of assimilation nutrients for valuable astaxanthin production with a concentration ranging from 2 to 4% of dry cell weight (DCW) [19]. Relevant studies demonstrated the relatively high removal efficiency of different antibiotics by *H. lacustris* and thus, it is theoretically feasible to regard *H. lacustris* as a promising microalgal strain of fluoroquinolone antibiotics removal [20,21]. Nevertheless, the removal efficiency of fluoroquinolone antibiotics via microalgae-based processes (such as *Chlorella vulgaris*, *Chrysosporum ovalisporum*, *Scenedesmus obliquus* and *Ourococcus multisporus*, *Micractinium resseri*) is in a range of 10–33%, which is not highly efficient for realistic application [18,22]. Therefore, the remediation improvement of fluoroquinolones by microalgae-based biological treatment is urgently needed via combination techniques to meet the realistic application.

Mixotrophic cultivation is able to drive microalgae to utilize and metabolize both organic and inorganic carbon sources simultaneously for constant growth. Compared with phototrophic (low biomass) and heterotrophic cultivation (high capital cost), mixotrophic cultivation could be an ideal and reasonable strategy to handle the challenges for microalgae-based fluoroquinolone antibiotics bioremediation. In addition, organic carbon source supply could also act as electron donors for the co-metabolism of micropollutants, which leads to the enhanced removal performance of pollutants [23,24]. For instance, it was found the effective co-metabolism of sulfamethoxazole by *Chlorella pyrenoidosa* with the aid of sodium acetate [24]. Similarly, the co-metabolism for removing ciprofloxacin of 2 mg/L was potentially achieved by *Chlorella* sp. under a glucose-based carbon source supplement [25]. Thus, the choice of a suitable and sufficient organic carbon source, acting as the electron donor for the co-metabolism of antibiotics, is the most important point to establish an efficient microalgae-based system. To the best of our knowledge, the feasibility and mechanism of co-metabolism of antibiotics by *H. lacustris* with the addition of an organic carbon source remain unclear, which is worth investigating.

To address these challenging issues, in this study, *H. lacustris* was employed to explore the removal capability of typical fluoroquinolone antibiotics with the aid of an organic carbon source supplement. Furthermore, the possible mechanistic interactions between the biodegradation of fluoroquinolone and microalgae-based co-metabolism were elucidated. Our findings provide novel insights into the green and low-carbon microalgae-based treatment of wastewater containing antibiotics for simultaneously promoting valuable product accumulation, with the mechanisms of microalgae-based pollutants co-metabolism at molecular levels.

2. Materials and methods

2.1. Algal strain and cultivation condition

Haematococcus lacustris (Chlorophyta, Strain No, CCMP-3127) was purchased from the Provasoli-Guillard National Center for Marine Algae and Microbiota (East Boothbay, USA). *H. lacustris* was maintained in 500 mL of Duran bottles fortified with 400 mL of 0.22 μm membrane-filtered Bold's Basal Medium (BBM medium) and placed in an artificial incubator under a continuous white light-emitting diode at 25 °C with a 12/12 h of the circadian rhythm. The light intensity of 120 $\mu mol \cdot m^{-2} \cdot s^{-1}$ was conducted during the macrozooid stage (0–12 days) and the light intensity of 400 $\mu mol \cdot m^{-2} \cdot s^{-1}$ was conducted during the hematocyst stage (12–16 days). The 0.22 μm membrane-filtered air-aerated system was applied through the whole cultivation period at a feed velocity of 15 mL/min. The initial cell density of *H. lacustris* for inoculation was 1×10^4 cells/mL.

2.2. Fluoroquinolone treatments of H. Lacustris

OFL (Purify >98%) and ENR (Purify >98%) were retrieved from Aladdin (Shanghai, China), and their relevant physicochemical properties were presented in Table S1. To prepare the biodegradation experiments of two typical fluoroquinolones, OFL and ENR were first dissolved into dimethyl sulfoxide (DMSO) at 5 mg/mL and 10 mg/mL as stocking solutions after adequate ultrasonication. Thereafter, the BBM cultivation medium of *H. lacustris* was exposed to varying concentrations of OFL and ENR at 1, 5, and 10 mg/L respectively. All experiments in this study were conducted with at least three biological replicates. Microalgal samples were collected at specific time points for further experimental analyses. The fluoroquinolone treatments supplied with organic carbon sources were described in Supporting Information.

2.3. Analytical methodologies

2.3.1. Analysis of fluoroquinolone and its intermediates

The quantification of fluoroquinolone was performed by high-performance liquid chromatography (HPLC, Agilent, USA) equipped with a C18 column (4.6×150 mm, 5 μm, Agilent, USA) using a UV detector at a 272 nm of detection wavelength. The intermediate of fluoroquinolones was identified using a Triple TOF 5600 Q-TOF liquid chromatography-tandem mass spectrometry (LC-MS/MS) in negative ionization mode with electrospray ionization (ESI). The protocols in detail were presented in Supporting Information.

2.3.2. Microalgal photosynthesis measurement

Photosynthetic parameters of *H. lacustris*, such as the maximum photochemical efficiency of photosystem II (Fv/Fm), the photosystem II-

based electron transport rate (ETR) and non-photochemical quenching (NPQ) during fluoroquinolone treatments supplemented with or without glycerol, were detected by a commercial phytoplankton photosynthesis analyzer (PhytoPAM II, Walz, Germany) following the manuals retrieved from the manufacturers. The CO_2 utilization efficiency and typical photosynthetic enzymes of *H. lacustris*, namely ribulose-1,5-bisphosphate carboxylase-oxygenase (RuBisCO) and carbonic anhydrase (CA), were measured fluoroquinolone treatments supplemented with or without glycerol during as per the protocols reported previously [17].

2.3.3. Microalgal biomass evaluation

H. lacustris cells at the scheduled time points were harvested by centrifugation at 4,000 rpm for 10 min. The pellets were subsequently transferred into pre-weighed 1.5 mL Eppendorf tubes and dried at 60 °C for 24 h. The biomass of *H. lacustris* was evaluated based on the dry cell weight which was determined gravimetrically at day 16.

2.3.4. Astaxanthin determination

The quantification of astaxanthin retrieved from *H. lacustris* harvested at day 16 was performed by high-performance liquid chromatography (HPLC, Waters, UK) equipped with a reversed-phase C18 column (Waters, UK) using a photodiode array detector at a 460 nm of detection wavelength. The protocols in detail were presented in Supporting Information.

2.3.5. Analysis of microalgal primary metabolites

The lipid content of *H. lacustris* was isolated by classical extraction protocol and subsequently determined gravimetrically. The carbohydrate of *H. lacustris* was extracted by classical phenol-sulfuric acid method and then detected by spectrophotometry. The protein of *H. lacustris* was isolated by RIPA lysis buffer (Beyotime, China) with phenylmethanesulfonyl fluoride (Beyotime, China) and quantified by a bicinchoninic acid (BCA) protein assay kit (Beyotime, China). The fatty acid composition of *H. lacustris* was transesterified into fatty acid methyl esters and analyzed by a gas chromatograph-mass spectrophotometer. The protocols in detail were presented in Supporting Information.

2.3.6. Analysis of residual glycerol in the culture medium

Glycerol in the culture medium was monitored by an HPLC (Agilent, USA) equipped with a Shodex SUGAR SH1011 column (8.0 mm I.D. × 300 mm, Showa Denko, Japan) using a refractive index detector. The protocols in detail were presented in Supporting Information.

2.3.7. Transcript analysis of microalgal genes

RNA samples were extracted using the Plant Total RNA Isolation Kit (Sangon, China) and then transcribed into cDNA using HiScript II Q RT SuperMix for qPCR (Vazyme, China). The transcript abundances of genes involved in the cellular metabolism process were determined by RT-qPCR analysis with primers listed in Table S2 using HiScript II Q RT SuperMix for qPCR (Vazyme, China) detected on a CFX96 Real-Time PCR Detection System (Bio-Rad, USA) to analyze the possible enzymes in fluoroquinolone biotransformation process mediated by *H. lacustris*. The protocols in detail were presented in Supporting Information.

2.3.8. Molecular docking and molecular dynamics simulation

The protocols in detail of molecular docking and molecular dynamics (MD) simulation were presented in Supporting Information.

2.4. Statistical analysis

All experiments were performed on at least biological triplicates and the data were expressed as mean ± standard deviation (SD) (n = 3). Statistical analyses were executed using GraphPad Prism 8. The detailed analyses were presented in Supporting Information.

3. Results and discussion

3.1. H. Lacustris exhibited the potential for fluoroquinolone antibiotics removal under a co-metabolism system

Microalgae exhibited a typical antibiotic tolerance and biodegradation capacity depending on different strain-antibiotic combinations [16]. Although the realistic fluoroquinolones on the risks to the aqueous environment are still in low concentrations ranging from ng to mg/L [7,8], the potential of antibiotic removal with a broad range of antibiotics should be considered by microalgae-based co-metabolism system due to the uncertain concentrations in the occurrence of aquatic antibiotics. Therefore, the maximum bioremediation capacity of *H. lacustris* was investigated in the presence of extremely high concentrations (1, 5, 10 mg/L) of OFL or ENR for the first time in this research. It was found that *H. lacustris* could potentially dissipate fluoroquinolone antibiotics with a wide concentration range (Fig. S1). A previous study has reported that *H. lacustris* was considered the most potent species with high removal efficiencies ranging between 42 and 100% with median value of 93% against antibiotics in a series of synthetic wastewater [20]. Furthermore, the abiotic removal factors revealed no or/and minor effects of hydrolysis and photolysis on antibiotic attenuation, which was in agreement with previous reports [20,26]. In particular, treatment with a low dose (1 mg/L) resulted in the highest removal efficiencies for OFL (100%) and ENR (89.71%) (Fig. S2), demonstrating that *H. lacustris* can be considered a feasible and promising alternative for the removal of fluoroquinolone antibiotics. It was surprising that, exposed to a high dose (5 or 10 mg/L) of antibiotics, the potential of *H. lacustris* was significantly inhibited with efficiencies of 37.83% and 21.85% for OFL removal, and 34.44% and 22.81% for ENR removal (Fig. S2), respectively, implying that the toxicity of the high dose of antibiotics to the growth of microalgae.

Recent studies have reported that a co-metabolism system supplied with organic substrates could be an efficient strategy to improve the tolerance to and biodegradation abilities of antibiotics [24,26,27]. It was demonstrated that factors, such as nutrient substrate, influence microalgal metabolism through co-metabolism, and consequently, play important roles in the upregulation of microalgae-based antibiotic removal [28]. Therefore, different carbon sources, such as $NaHCO_3$, glycerol, acetate, and glucose using a uniform chemical oxygen demand at 10 g/L equivalent amount, were employed to assess the removal effect of *H. lacustris* on the response to high concentrations of fluoroquinolones. As shown in Fig. 1A and B, glycerol addition in the *H. lacustris* cultures caused a notable increase in the removal efficiency of antibiotics compared with other carbon sources, which showed that the microalgae-based co-metabolism was activated by glycerol for accelerating the biodegradation of antibiotics. Previous reports have demonstrated that the additional substrates act as electron donors for the pollutant co-metabolic biodegradation [24]. The level of intracellular pyruvate exhibited a remarkable increase in *H. lacustris* in the presence of high concentrations of fluoroquinolones (Fig. S3). Based on these results, it was speculated that the external carbon source activated microalgae to form products from glycerol metabolisms, such as pyruvate, which is a key component in synergistic metabolism and an excellent electron donor for biodegrading antibiotics [29].

Liang et al. reported that the co-metabolism system of pollutants depended on the added amount of external carbon source [30]. Accordingly, a series concentration range of glycerol was added into *H. lacustris* cultures exposure to 10 mg/L OFL or ENR. As shown in Fig. 1C and D, *H. lacustris* exhibited a higher removal efficiency of antibiotics when exposed to glycerol between 0.05 M and 0.1 M. The dose-response correlation relates to the exposure concentrations of glycerol. Generally, higher doses lead to enhanced responses to antibiotic removal [30]. In particular, 0.075 M of glycerol achieved the maximum removal efficiency of OFL under co-metabolism, at the same time, 0.05 M was considered as most suitable glycerol concentration for

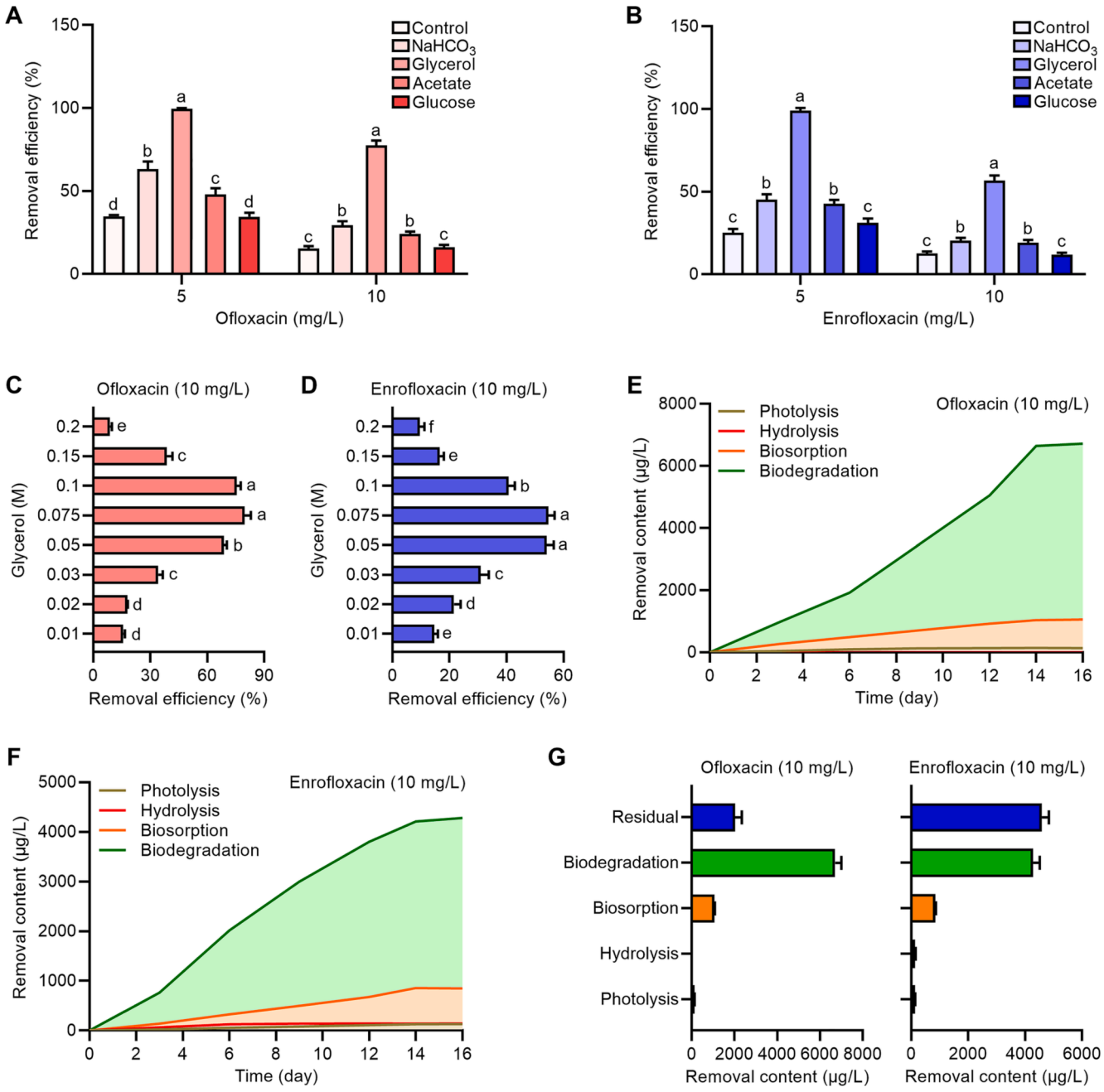

Fig. 1. Removal summary of fluoroquinolones by co-metabolism using *H. lacustris*. (A-B) Removal efficiency of OFL and ENR with different carbon sources at 10 g/L equivalent amount of chemical oxygen demand. (C-D) Removal efficiency of OFL and ENR with a series range of glycerol. (E-F) Removal content of OFL and ENR during the treatment period. (G) Detailed removal content of OFL and ENR. Error bars represent the standard deviations of measurements of samples ($n \geq 3$). Different lowercase letters on the column bars indicate significant differences at $p < 0.05$.

biodegrading ENR under co-metabolism due to the highest removal ability. Moreover, the removal efficiency of *H. lacustris* was observed to be inhibited with a higher concentration of glycerol (0.15 M and 0.2 M), which may be related to the inhibition of microalgae with the addition of high concentrations of carbon sources [31]. As a result, 0.075 M and 0.05 M of glycerol were selected for the further biodegradation of OFL and ENR in the subsequent experiments, respectively.

The biodegradation trend of fluoroquinolones by co-metabolism mediated by *H. lacustris* was initiated at the beginning during the period of co-metabolism with a slow rate (Fig. 1E and F), suggesting that a lag or adaptation phase of antibiotic removal existed in the microalgae-based co-metabolism system. A previous report also demonstrated a similar lag phenomenon in microorganisms during the removal of ozonation products of pharmaceuticals [32]. Furthermore, the biodegradation trend subsequently achieved the maximum rate during the log phase and turned to a plateau during the astaxanthin-accumulation phase. Compared to the residual antibiotics, the removal content of OFL and ENR by biotic behaviors (i.e., biodegradation, biosorption) reached a maximum content of 7.77 mg/L and 5.13 mg/L, respectively (Fig. 1G, Tables S3). Specifically, the biodegradation efficiency of fluoroquinolone co-metabolism mediated by *H. lacustris* was 67.14% and 42.83%, respectively. It can be seen that the removal rate of fluoroquinolones by *H. lacustris* was accelerated to varying degrees when glycerol was added to the medium (Fig. S1), indicating that co-metabolism triggered an increase in the amount of antibiotic removal [24,27]. The biodegradation kinetics of OFL and ENR was performed

using a pseudo-first-order model (Table S4). As expected, the correlation coefficient (R^2) was 0.931 and 0.971, suggesting that the fluoroquinolone removal exhibited the goodness of fit to the pseudo-first-order kinetic model. The constant (k, d^{-1}) was 0.0766 and 0.1056, indicating a high biodegradation rate of fluoroquinolones during the co-metabolism mediated by *H. lacustris*. Taken together, it was postulated that biotic processes by *H. lacustris* would be the main behavior responsible for the removal of fluoroquinolones in the presence of external glycerol.

3.2. Glycerol supplement stimulated biochemical characterizations of *H. Lacustris* under the fluoroquinolones co-metabolism system

As shown in Fig. S4 and discussion in Supporting Information, it is reasonable to conclude that glycerol-involved co-metabolism of fluoroquinolones enhanced the capacity of CO_2 entering into microalgae for increasing photosynthetic performance through the Calvin-Benson-Bassham cycle and the CO_2 fixation, and thereby improving the biodegradation abilities of *H. lacustris*. Carbohydrates are formed in microalgae by photosynthesis, and thus we further analyzed the carbohydrate content during the cultivation period. As expected, the carbohydrate of *H. lacustris* achieved a higher content with glycerol (Fig. 2A), implying that a higher photosynthetic performance owing to glycerol supplement contributed to the accumulation of carbohydrate. In contrast, glycerol as a carbon source for another microalga species *Phaeodactylum tricornutum* hardly devoted to the biosynthesis of carbohydrate [33]. Similarly, exogenous glycerol also did not change the biomass of *H. pluvialis* [34]. A previous report might provide a possible explanation that antibiotics might be a carbon source and consequently improve the cellular carbohydrate reserves for cell growth [35]. Specifically, the carbohydrate content tended to decline after day 6. One possible explanation for the sudden decline of carbohydrates is that the decrease in carbohydrate mainly contributed to the growth of *H. lacustris*. On the other hand, the protein content of *H. lacustris* also increased significantly (Fig. 2F), suggesting that the carbon flux was redirected into protein biosynthesis from carbohydrate biosynthesis after 6 days. Furthermore, the residual glycerol content in the culture medium was found to be consumed at a stable rate during the macrozooid stage (0–12 days) and turned into a quick consumption mode during the haematocyst stage (12–16 days) (Fig. 2B). Glycerol was proven to accelerate astaxanthin and lipids accumulation of *H. pluvialis* [34]. Hence, we speculated that at the macrozooid stage, the

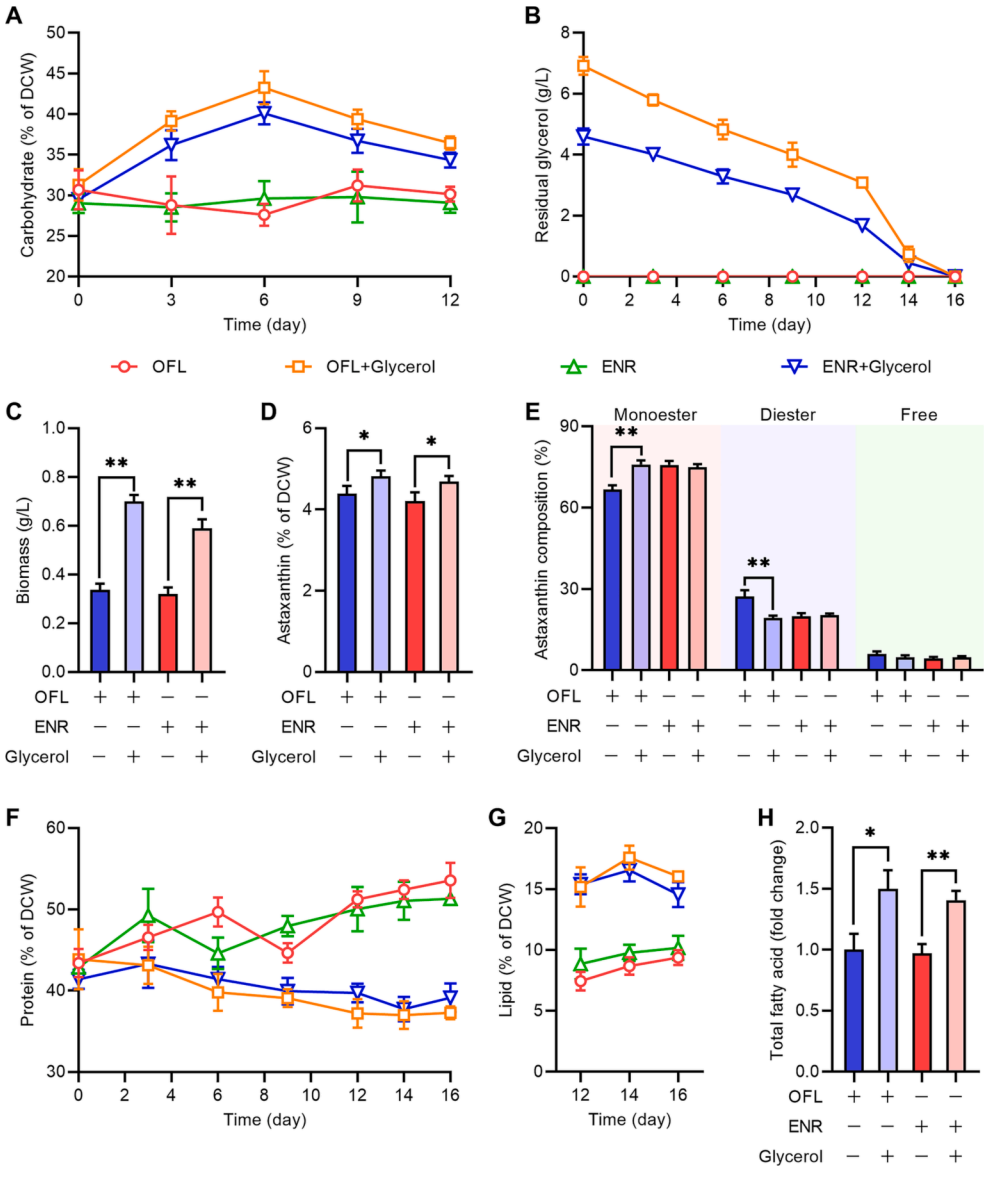

Fig. 2. Biochemical properties of *H. lacustris* under the fluoroquinolones co-metabolism system. (A) Carbohydrate content during the macrozooid period. (B) Residual glycerol content in culture medium during the treatment period. (C) Biomass content. (D) Astaxanthin content. (E) Astaxanthin profiles. (F) Protein content during the treatment period. (G) Lipid content during the haematocyst period. (H) Total fatty acid content. The mark '+' represents that the chemical was added to the culture medium. The mark '-' represents that the chemical was not added to the culture medium. Error bars represent the standard deviations of measurements of samples ($n \geq 3$). Significant differences between the control and treatment groups are indicated at the $p < 0.01$ (**) and $p < 0.05$ (*) level.

consumption of glycerol turned to the contribution of antibiotic removal; meanwhile, the consumption of glycerol at the haematocyst stage switched to the dedication of microalgae-based valuable product accumulation. Zhang et al. demonstrated that the microalgae-based co-metabolism of antibiotics could be enhanced by adding an external carbon source, thereby promoting microalgal biomass [36]. A similar result of biomass has also occurred in this study (Fig. 2C), implying that microalgal-mediated biodegradation utilizes organic contaminants as carbon sources for biomass accumulation with a corresponding increase in antibiotic removal.

Moreover, the astaxanthin content of *H. lacustris* cultures with glycerol was higher than that in cultures without glycerol at the haematocyst stage (Fig. 2D). This shows that the glycerol supplementation on *H. lacustris* plays a critical role in accelerating the accumulation of astaxanthin, which is in accordance with the previous report [34]. In addition, as astaxanthin monoesters are more responsible for bioavailability than other astaxanthin forms, we determined the ester profile of astaxanthin in *H. lacustris* cultures. As shown in Fig. 2E, the ratios of astaxanthin esters were changed significantly by the supplement of glycerol, with upregulated monoesters and downregulated diesters. This suggests that the glycerol-involved biodegradation of fluoroquinolones recalibrated the formation of the ester towards monoesters in *H. lacustris* cultures. The protein content of *H. lacustris* cultures with glycerol was significantly decreased during the whole antibiotic treatment period (Fig. 2F), suggesting that *H. lacustris* cultures with glycerol caused carbon precursors to be directed towards carbohydrate biosynthesis rather than towards protein biosynthesis at the macrozooid stage. Furthermore, the content of lipids was remarkably increased at the haematocyst stage (Fig. 2G), demonstrating glycerol-involved co-metabolism system redirected carbon metabolism to lipogenesis at the microalgal stationary phase [17,31]. It was reported that the astaxanthin esterification process in *Haematococcus* is accompanied by fatty acid biosynthesis [37]. In keeping with this trend, the fatty acid level of *H. lacustris* was elevated by using glycerol (Fig. 2H). Moreover, fatty acid profiles such as C16:0, C16:3, C18:2 and C18:3 were shown as the major fatty acids with significant changes in the proportions (Fig. S5), indicating the treatment of glycerol caused the change of fatty acid profiles at the haematocyst stage. These findings are in agreement with our hypothesis that the enhanced pyruvate caused by glycerol addition can be converted into acetyl-CoA as precursors for fatty acid biosynthesis, thereby resulting in the simultaneous increase of astaxanthin and lipid accumulation.

3.3. *Molecular responses of H. Lacustris provided preliminary interactions between glycerol supply and fluoroquinolones co-metabolism*

Previous studies have demonstrated that molecular analyses of microalgae could reveal the potential mechanism of responses by numerous treatments [19,31]. As shown in Fig. 3A, the key genes involved in RuBisCO biosynthesis were constantly decreased, at the

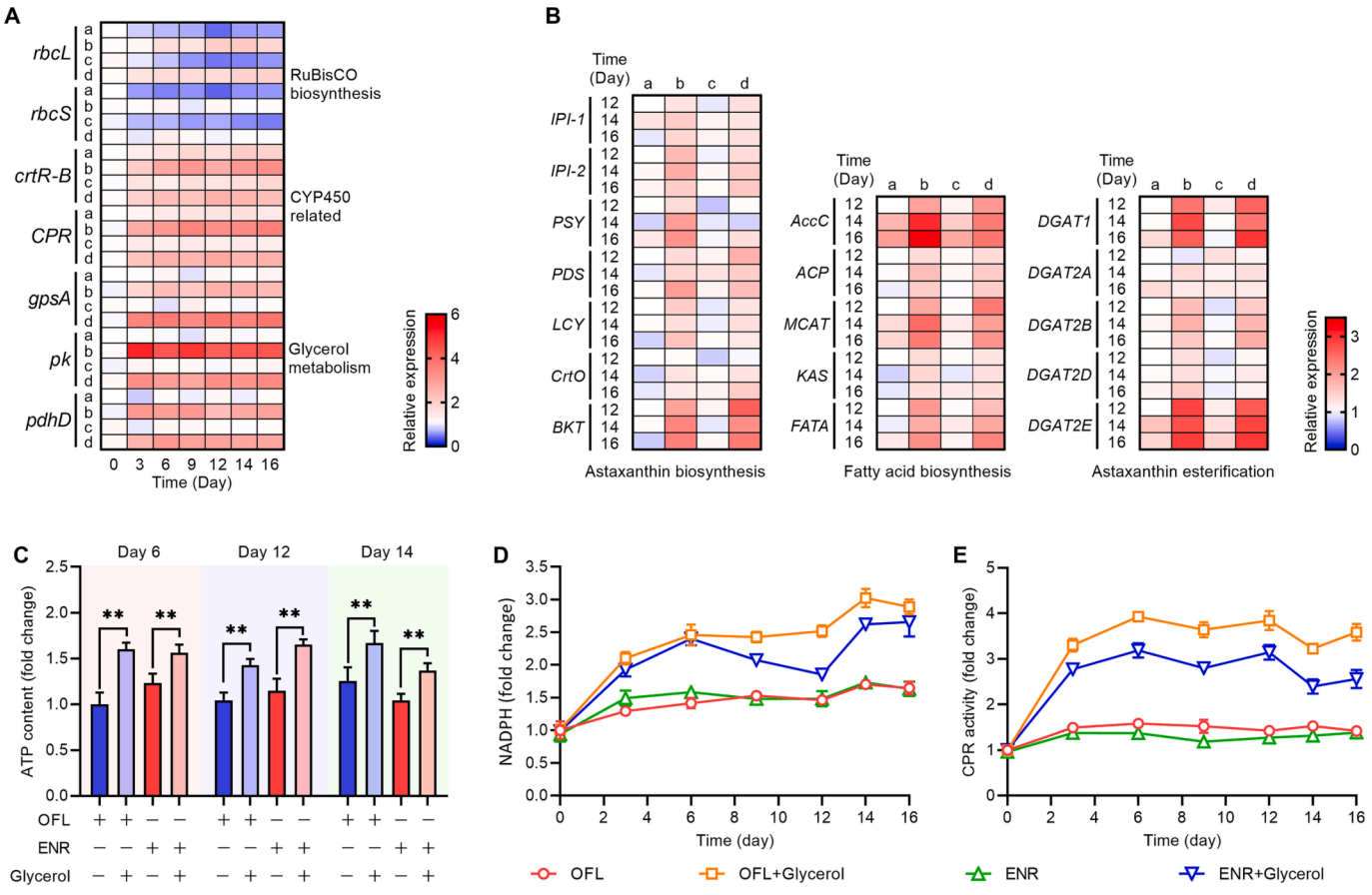

Fig. 3. Molecular responses of *H. lacustris* under the fluoroquinolones co-metabolism system. (A) RT-qPCR analyses of RuBisCO biosynthesis, CYP450 related and glycerol metabolism during the treatment period. (B) RT-qPCR analyses of astaxanthin biosynthesis, fatty acid biosynthesis and astaxanthin esterification during the haematocyst period. 'a' represents the group of OFL treatment, 'b' represents the group of OFL treatment added with glycerol, 'c' represents the group of ENR treatment, 'd' represents the group of ENR treatment added with glycerol. (C) ATP content. The mark '+' represents that the chemical was added to the culture medium. The mark '-' represents that the chemical was not added to the culture medium. (D) NADPH content. (E) CPR enzymatic activity. Error bars represent the standard deviations of measurements of samples ($n \geq 3$). Significant differences between the control and treatment groups are indicated at the $p < 0.01$ (**) and $p < 0.05$ (*) level.

same time, the glycerol supply significantly improved the expression level. It was reported that cytochromes P450 (CYP450), one of the most effective defenders in microalgae, plays a critical role in the biodegradation of antibodies [38]. As expected, two CYP450-related genes were found to be continuously increased in the presence of glycerol (Fig. 3A), suggesting that the P450 enzyme system may be the important catalytic enzyme. Similarly, as shown in Fig. 3E, it was found that the enzymatic activity of cytochrome P450 reductase (CPR) was similar to the qPCR result of CPR. Changes in the expression of key genes related to glycerol metabolism of *H. lacustris* also illustrated the positive impact of glycerol on cells (Fig. 3A). The expression level of genes related to astaxanthin accumulation was shown in Fig. 3B, demonstrating that glycerol supplementation might be responsible for astaxanthin biosynthesis, fatty acid biosynthesis, and astaxanthin esterification, which provided certain explanations for the effective astaxanthin accumulation of *H. lacustris* under the fluoroquinolones co-metabolism system. In addition, the results shown in Fig. S6 and discussion in Supporting Information demonstrated that glycerol activated the enzymatic ROS-scavenging capacities of *H. lacustris*, thereby leading to ROS elimination, with the latter accounting for the accumulation of astaxanthin.

It was found that adenosine triphosphate (ATP) energy is assigned to maintain cellular antioxidant capacities, thereby ameliorating the oxidative damage caused by ROS generation [39]. Compared with *H. lacustris* cultures without glycerol, glycerol supply to *H. lacustris* showed a stable and significant increase in ATP content (Fig. 3C). This suggests that an increased ATP content might be attributable to ROS elimination. In addition, excessive ATP content was reported to improve the capacities of pollutant removal in wastewater [40]. Intriguingly, as a consequence of the amelioration of oxidative damage, the reduced nicotinamide adenine dinucleotide phosphate (NADPH) content was significantly higher in *H. lacustris* cultures with glycerol (Fig. 3D). Apart from the alleviation function of NADPH to oxidative stress, NADPH also exhibited a major reducing equivalent for the biosynthesis of microalgae-based metabolites [19]. Based on these data, thus, it is assumed that the increase of ATP and NADPH stimulated by glycerol may provide enough reducing equivalents for concurrently alleviating oxidative damage and improving microalgae-based products.

3.4. Identification of proposed metabolites of fluoroquinolones under the microalgae-based co-metabolism system

In order to understand the co-metabolism of fluoroquinolones, the related biotransformation products of OFL and ENR under the microalgae-based co-metabolism system were identified by LC-MS/MS (Figs. S7-S8, Table S5-S6). Moreover, three possible pathways related to OFL biodegradation, and three proposed pathways related to ENR biodegradation were presented in Fig. 4. Specifically, in Pathway I, OFL was converted to OFL-M1 through the processes of deoxygenation, dehydration and demethylation, and subsequently converted to OFL-M2 via the removal of the piperazine ring and the addition of a ketone group. In Pathway II, OFL was converted to OFL-M3 through the processes of demethylation and decarboxylation. In Pathway III, OFL was transformed into OFL-M4 by demethylation and deoxygenation. OFL-M4 converted to OFL-M5 via the processes of defluorination, the

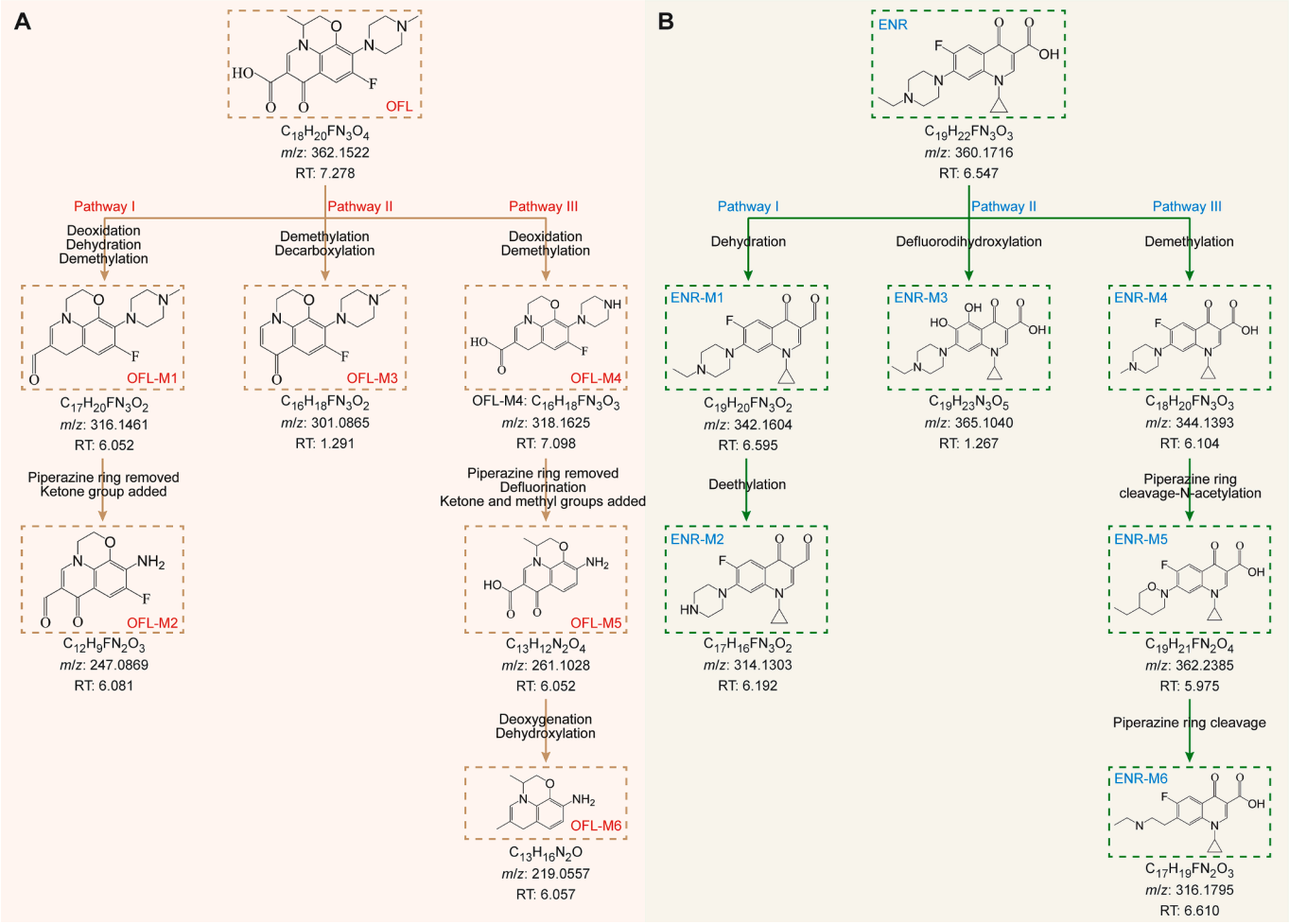

Fig. 4. Proposed biodegradation pathways of fluoroquinolones by *H. lacustris* under the co-metabolism system. (A) OFL biodegradation pathways. (B) ENR biodegradation pathway.

removal of the piperazine ring, and the addition of a keto group and a methyl group. OFL-M5 transformed into OFL-M6 by deoxygenation and dehydroxylation. For ENR biodegradation, Pathway I of ENR contained two compounds, including ENR-M1 by dehydration and ENR-M2 by deethylation. In Pathway II, ENR was directly converted to ENR-M3 by defluorodihydroxylation. In Pathway III, ENR was transformed into ENR-M4, ENR-M5 and ENR-M6 through demethylation, piperazine ring cleavage-N-acetylation and piperazine ring cleavage step by step. Although a total of 12 biodegraded compounds was identified by LC-MS/MS, which can reflect the possible biodegradation pathways of fluoroquinolones under the microalgae-based co-metabolism system, some smaller molecular weight biodegraded products were not identified because of the detection limit. Moreover, it was speculated that most fluoroquinolones might be biodegraded into substrates or intermediates for the metabolism of *H. lacustris* to achieve high contents of astaxanthin and lipid.

Through the analyses of the above biodegradation pathways, the formation of metabolites during fluoroquinolones biodegradation by *H. lacustris* may be catalyzed by the species-specific enzyme system of microalgae for detoxification in response to antibiotics [41]. The detoxification metabolism by CYP450 enzymes may be responsible for the biotransformation of antibiotics [42,43], which is consistent with our qPCR data shown in Fig. 3A. Moreover, CYP450 enzymes, such as monooxygenases, dioxygenases, hydroxylases, carboxylases, decarboxylases and etc., are generally involved in the hydrolysis, oxidation, and reduction reactions for biodegrading antibiotics [42]. Therefore, we speculated that CYP450 enzymes are involved in the biotransformation of OFL and ENR to achieve detoxification of fluoroquinolones by co-metabolism of *H. lacustris*. There have been several reports on the degradation of OFL and ENR; however, the formed metabolites are quite different [44,45]. Although the degraded products from fluoroquinolones are different depending on the species of the organism, the role of CYP450 enzymes is irreplaceable [46,47]. The results shown in Table S7 and discussion in Supporting Information demonstrated that the toxicity evaluation of metabolites formed from fluoroquinolone biodegradation. Taken together, these data plausibly explained the biodegradation metabolites and also proposed pathways of OFL and ENR co-metabolism by *H. lacustris* with glycerol with the aid of CYP450 enzymes.

3.5. The possible mechanistic interactions between the biodegradation of fluoroquinolone and CYP450 enzymes

A detailed understanding of the molecular interactions between fluoroquinolone and CYP450 enzymes still requires further investigation. Two CYP450 enzymes, including β-carotene hydroxylase (CrtR-B) and CPR, were selected for further analyses of the mechanistic interactions between the biodegradation of fluoroquinolone and CYP450 enzymes. The results of molecular docking revealed hydrogen bonds between CrtR-B and OFL along with ENR, respectively (Fig. S9A and B). Furthermore, there were five hydrogen bonds between CPR and OFL, and three hydrogen bonds between CPR and ENR (Fig. S9C and D, Table S8). This suggests the tight binding of fluoroquinolones to CPR active pocket, thereby leading to the higher stability of CPR-OFL/ENR complexes than that of CrtR-B-OFL/ENR. In addition, the CYP450 inhibition assay demonstrated that CPR-mediated activation might be responsible for fluoroquinolones biodegradation under the microalgae-based co-metabolism system (Fig. S10). Therefore, CPR was selected for further analyses. It was well known that CPR has the ability to metabolize exogenous compounds [48,49]; however, the underlying molecular mechanism of CPR-mediated biodegradation of fluoroquinolones still remains unknown. Therefore, we predicted the possible metabolic sites of CPR-OFL/ENR complexes based on molecular docking and MD simulation to analyze the potential binding mechanism.

Root-mean-square deviation (RMSD) is a prominent structural and dynamic parameter for investigating conformational stability [50]. As shown in Fig. 5A and B, the RMSD values of CPR-OFL and CPR-ENR did not change after 15 ns and 14 ns, respectively, demonstrating that the complex conformation of CPR-fluoroquinolones appeared to reach convergence. Furthermore, the RMSD values of CPR-OFL/ENR complexes were similar to that of CPR, suggesting that a strong binding existed between the OFL/ENR and CPR. Radius of gyration (Rg) acts as one key indicator of the protein structure compactness, which can reflect the stable conformation status of the complexes [51]. It was reported that the Rg value of CPR-OFL gradually decreased until 14 ns to reach relative stability (Fig. 5C); meanwhile, the Rg value of CPR-ENR rose at first and turned to decrease after 8 ns (Fig. 5D). Furthermore, the fluctuations of the Rg values of CPR-OFL/ENR and CPR exhibited strong consistency and converged to equilibrium, implying that the CPR-OFL/ENR complexes were well-folded. Root-mean-square fluctuation (RMSF) represents the fluctuation of each atom or residue within a definite time period during the protein dynamic simulation, which reflects the flexibility of protein during the MD simulation [52]. It was shown that the RMSF value of CPR-OFL is higher than that of CPR (Fig. 5E), indicating that the binding of OFL induced to an increase of flexibility to adjust to a stable conformation of CPR-OFL complex. Moreover, the RMSF value of CPR-ENR demonstrated a slight decrease in residue numbers of 49–62 and 81–123 (Fig. 5F), implying the restricted movement of the CPR-ENR complex might be related to the tight bind between CPR and ENR (Supplementary Movies 1 and 2). These data were in agreement with the results of MD evolution shown in Fig. S11 and discussion in Supporting Information.

To clearly clarify the interactions between CPR and OFL/ENR, MM/PBSA method was performed to calculate the binding free energy based on the values of van der Waals interactions, electrostatic interactions, polar solvation, and non-polar solvation interactions [52]. As shown in Tables S9 and S10, the values of binding free energies ($\Delta G_{binding}$) of CPR-OFL and CPR-ENR indicated that OFL and ENR can easily and tightly bound to CPR. It was reported that the residues less than −1.0 kcal/mol of the binding energy contribution are considered key residues for investigating molecular recognition of small molecular ligands by proteins [53]. As expected, the contribution energy of CPR residues to OFL or ENR was less than −1.0 kcal/mol in several residue numbers (Fig. 5G and H). Specifically, Leu6, Cys84, Ala112, Tyr122, Val123, and Met154 were found to be potential residues for the contribution of binding free energy (Fig. 5I), while Cys84, Asp121, and Val123 were found to form hydrogen bonds to efficiently bind to CPR (Fig. 5J). As shown in Fig. 5K and L, Pro51, Arg85, Ala112, Tyr122, Val123, and His153 were considered the main contributions to binding energy, and Ala112, Ser114, and Val123 were found to participate in the formation of hydrogen bonds, resulting in efficient and tight binding of ENR to CPR. Taken together, OFL and ENR might insert into CPR binding pocket to ultimately form an effective and tight binding conformation for the biodegradation of antibiotics in microalgae.

4. Conclusion

In this study, the feasibility of alga *H. lacustris* for the synergistic performance of fluoroquinolones was systematically investigated under a co-metabolism system. The retrieved results reveal that *H. lacustris* exhibited good potential for antibiotics removal in 1 mg/L of fluoroquinolone. Glycerol as an excellent substrate improved the capabilities of physiological and oxidative responses of *H. lacustris*, which are crucial for fluoroquinolone removal. Consequently, the biodegradability of *H. lacustris* for extremely high concentrations of antibiotics driven by glycerol was improved significantly, accompanied by the simultaneous increase of microalgal astaxanthin and lipid. Molecular analyses and MD simulations indicated that CYP450 enzymes, especially CRP, were able to efficiently and tightly bind to fluoroquinolones while contributing to the biodegradation of fluoroquinolones by *H. lacustris*. In summary, we demonstrate how the alga *Haematococcus lacustris* could biodegrade fluoroquinolones under a glycerol-involved co-metabolism system for

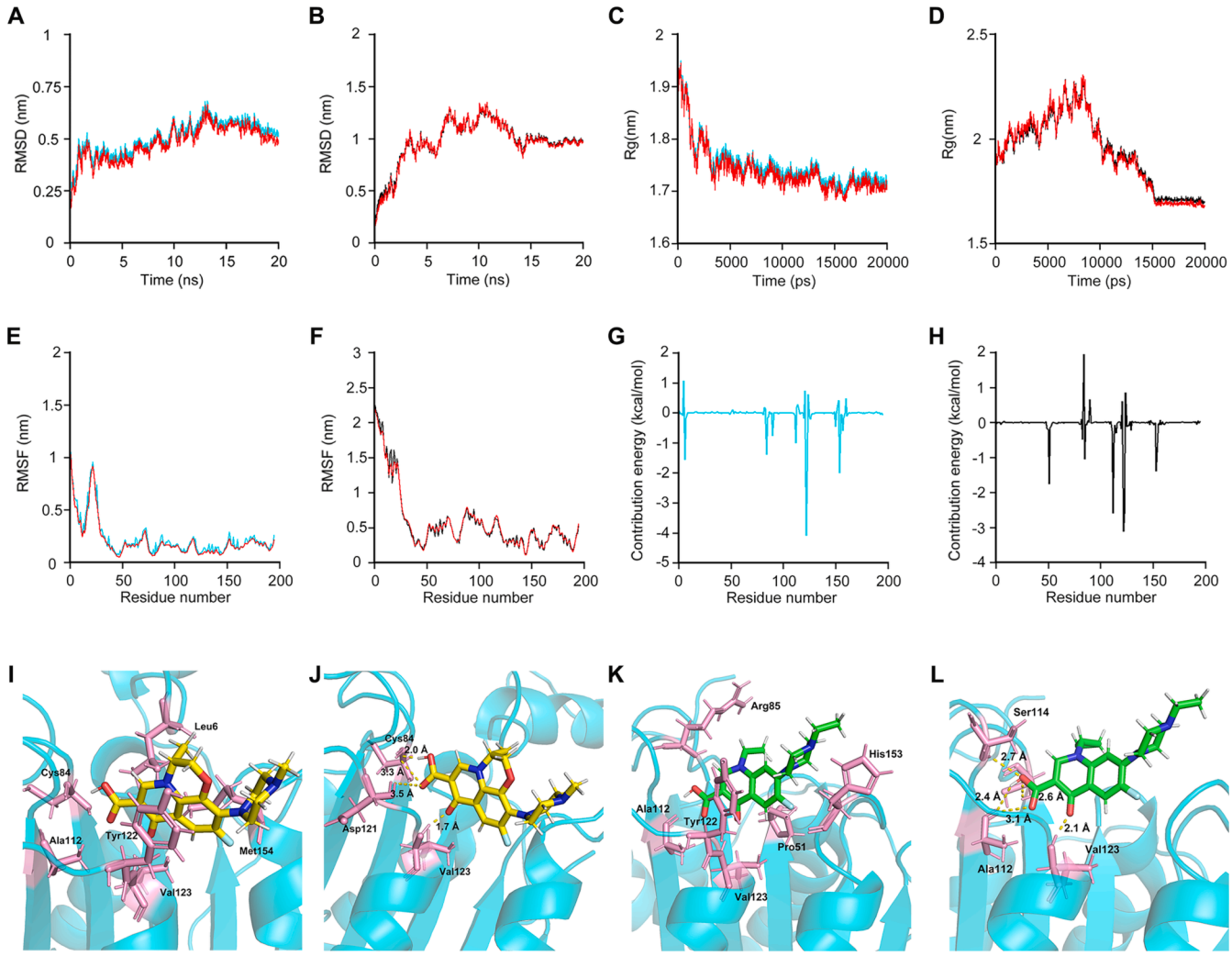

Fig. 5. MD simulation the binding process of CPR with OFL and ENR. CPR-OFL (cyan), CPR-ENR (black), CPR (red). (A-B) RMSD values of CPR, CPR-OFL and CPR-ENR. (C-D) Rg values of CPR, CPR-OFL and CPR-ENR. (E-F) RMSF values of CPR, CPR-OFL and CPR-ENR. (G-H) The contribution of individual residues of CPR to the total binding energy toward OFL and ENR during MD simulation. (I-J) Key energy contributing residues and hydrogen bonding of CPR and OFL. (K-L) Key energy contributing residues and hydrogen bonding of CPR and ENR.

simultaneously increasing astaxanthin and lipid production. This study provides a novel and low-carbon strategy for the sustainable biodegradation of extremely high concentrations of antibiotic pollution accompanied by valuable product accumulation of microalgae. Although the realistic fluoroquinolones on the risks to the environment are still in ng to mg/L levels, the broad biodegradability of antibiotics is needed in this microalgae-based co-metabolism system due to the uncertain concentrations in the occurrence of aquatic antibiotics. Of course, it will be worthy of further study to confirm the realistic application of this microalgae-based co-metabolism system in real antibiotic-containing wastewater in the future.

CRediT authorship contribution statement

Xiang Wang: Conceptualization, Methodology, Data curation, Writing – original draft, Project administration. **Zhong-Hong Zhang:** Methodology, Data curation, Visualization. **Kuan-Kuan Yuan:** Methodology, Data curation, Validation. **Hui-Ying Xu:** Methodology, Validation. **Guo-Hui He:** Resources, Validation, Investigation. **Libin Yang:** Resources, Visualization. **Joseph Buhagiar:** Data curation, Writing – review & editing. **Wei-Dong Yang:** Resources. **Yalei Zhang:** Writing – review & editing, Project administration. **Carol Sze Ki Lin:** Writing – review & editing. **Hong-Ye Li:** Writing – review & editing, Supervision.

Declaration of Competing Interest

The authors declare that they have no known competing financial interests or personal relationships that could have appeared to influence the work reported in this paper.

Data availability

Data will be made available on request.

Acknowledgments

This work was supported by the Natural Science Foundation of China (51908244), Guangdong Basic and Applied Basic Research Foundation (2023A1515012314) and the China Postdoctoral Science Foundation (2018M643363, 2019T120789).

Appendix A. Supplementary data

Supplementary data to this article can be found online at https://doi.org/10.1016/j.cej.2023.142770.

References

[1] X. Yin, E.G. Dudley, C.N. Pinto, N.M. M'Ikanatha, Fluoroquinolone sales in food animals and quinolone resistance in non-typhoidal *Salmonella* from retail meats: United States, 2009–2018, J. Glob. Antimicrob. Resist. 29 (2022) 163–167, https://doi.org/10.1016/j.jgar.2022.03.005.

[2] D.J. Buehrle, M.M. Wagener, C.J. Clancy, Outpatient fluoroquinolone prescription fills in the United States, 2014 to 2020: Assessing the impact of Food and Drug Administration safety warnings, Antimicrob. Agents Chemother. 65 (7) (2021) e00151–e00221, https://doi.org/10.1128/AAC.00151-21.

[3] A. Sankar, K.M. Swanson, J. Zhou, A.B. Jena, J.S. Ross, N.D. Shah, P. Karaca-Mandic, Association of fluoroquinolone prescribing rates with black box warnings from the US Food and Drug Administration, JAMA Netw. Open 4 (12) (2021) e2136662–e, https://doi.org/10.1001/jamanetworkopen.2021.36662.

[4] W. Wang, W. Zhang, H. Liang, D. Gao, Occurrence and fate of typical antibiotics in wastewater treatment plants in Harbin, North-east China, Front. Environ. Sci. Eng. 13 (3) (2019) 34, https://doi.org/10.1007/s11783-019-1118-3.

[5] X. You, D. Wu, H. Wei, B. Xie, J. Lu, Fluoroquinolones and β-lactam antibiotics and antibiotic resistance genes in autumn leachates of seven major municipal solid waste landfills in China, Environ. Int. 113 (2018) 162–169, https://doi.org/10.1016/j.envint.2018.02.002.

[6] R. Zhang, K. Yu, A. Li, Y. Wang, X. Huang, Antibiotics in corals of the South China Sea: Occurrence, distribution, bioaccumulation, and considerable role of coral mucus, Environ. Pollut. 250 (2019) 503–510, https://doi.org/10.1016/j.envpol.2019.04.036.

[7] A. Rusu, G. Hancu, V. Uivaroşi, Fluoroquinolone pollution of food, water and soil, and bacterial resistance, Environ. Chem. Lett. 13 (1) (2015) 21–36, https://doi.org/10.1007/s10311-014-0481-3.

[8] C. Rutgersson, J. Fick, N. Marathe, E. Kristiansson, A. Janzon, M. Angelin, A. Johansson, Y. Shouche, C.-F. Flach, D.G.J. Larsson, Fluoroquinolones and qnr genes in sediment, water, soil, and human fecal flora in an environment polluted by manufacturing discharges, Environ. Sci. Technol. 48 (14) (2014) 7825–7832, https://doi.org/10.1021/es501452a.

[9] P. Mathur, D. Sanyal, D.L. Callahan, X.A. Conlan, F.M. Pfeffer, Treatment technologies to mitigate the harmful effects of recalcitrant fluoroquinolone antibiotics on the environ- ment and human health, Environ. Pollut. 291 (2021), 118233, https://doi.org/10.1016/j.envpol.2021.118233.

[10] C.M. Teglia, F.A. Perez, N. Michlig, M.R. Repetti, H.C. Goicoechea, M.J. Culzoni, Occurrence, distribution, and ecological risk of fluoroquinolones in rivers and wastewaters, Environ. Toxicol. Chem. 38 (10) (2019) 2305–2313, https://doi.org/10.1002/etc.4532.

[11] M.-K. Jin, Q. Zhang, W.-L. Zhao, Z.-H. Li, H.-F. Qian, X.-R. Yang, Y.-G. Zhu, H.-J. Liu, Fluoroquinolone antibiotics disturb the defense system, gut microbiome, and antibiotic resistance genes of *Enchytraeus crypticus*, J. Hazard. Mater. 424 (2022), 127509, https://doi.org/10.1016/j.jhazmat.2021.127509.

[12] I. Michael, L. Rizzo, C.S. McArdell, C.M. Manaia, C. Merlin, T. Schwartz, C. Dagot, D. Fatta-Kassinos, Urban wastewater treatment plants as hotspots for the release of antibiotics in the environment: A review, Water Res. 47 (3) (2013) 957–995, https://doi.org/10.1016/j.watres.2012.11.027.

[13] W. Zieliński, E. Korzeniewska, M. Harnisz, J. Drzymała, E. Felis, S. Bajkacz, Wastewater treatment plants as a reservoir of integrase and antibiotic resistance genes – An epidemiological threat to workers and environment, Environ. Int. 156 (2021), 106641, https://doi.org/10.1016/j.envint.2021.106641.

[14] B.L. Phoon, C.C. Ong, M.S. Mohamed Saheed, P.-L. Show, J.-S. Chang, T.C. Ling, S. S. Lam, J.C. Juan. Conventional and emerging technologies for removal of antibiotics from wastewater. J. Hazard. Mater. 400. (2020). 122961. https://doi.org/10.1016/j.jhazmat.2020.122961.

[15] A.S. Oberoi, Y. Jia, H. Zhang, S.K. Khanal, H. Lu, Insights into the fate and removal of antibiotics in engineered biological treatment systems: A critical review, Environ. Sci. Technol. 53 (13) (2019) 7234–7264, https://doi.org/10.1021/acs.est.9b01131.

[16] L. Leng, L. Wei, Q. Xiong, S. Xu, W. Li, S. Lv, Q. Lu, L. Wan, Z. Wen, W. Zhou, Use of microalgae based technology for the removal of antibiotics from wastewater: A review, Chemosphere 238 (2020), 124680, https://doi.org/10.1016/j.chemosphere.2019.124680.

[17] X. Wang, Z.-H. Qin, T.-B. Hao, G.-B. Ye, J.-H. Mou, S. Balamurugan, X.-Y. Bin, J. Buhagiar, H.-M. Wang, C.S.K. Lin, W.-D. Yang, H.-Y. Li, A combined light regime and carbon supply regulation strategy for microalgae-based sugar industry wastewater treatment and low-carbon biofuel production to realise a circular economy, Chem. Eng. J. 446 (2022), 137422, https://doi.org/10.1016/j.cej.2022.137422.

[18] Q. Xiong, L.-X. Hu, Y.-S. Liu, J.-L. Zhao, L.-Y. He, G.-G. Ying, Microalgae-based technology for antibiotics removal: From mechanisms to application of innovational hybrid systems, Environ. Int. 155 (2021), 106594, https://doi.org/10.1016/j.envint.2021.106594.

[19] X. Wang, J.-H. Mou, Z.-H. Qin, T.-B. Hao, L. Zheng, J. Buhagiar, Y.-H. Liu, S. Balamurugan, Y. He, C.S.K. Lin, W.-D. Yang, H.-Y. Li, Supplementation with rac-GR24 facilitates the accumulation of biomass and astaxanthin in two successive stages of *Haematococcus pluvialis* cultivation, J. Agric. Food Chem. 70 (15) (2022) 4677–4689, https://doi.org/10.1021/acs.jafc.2c00479.

[20] C. Kiki, A. Rashid, Y. Wang, Y. Li, Q. Zeng, C.-P. Yu, Q. Sun, Dissipation of antibiotics by microalgae: Kinetics, identification of transformation products and pathways, J. Hazard. Mater. 387 (2020), 121985, https://doi.org/10.1016/j.jhazmat.2019.121985.

[21] C. Kiki, X. Ye, X. Li, B. Adyari, A. Hu, D. Qin, C.-P. Yu, Q. Sun, Continuous antibiotic attenuation in algal membrane photobioreactor: Performance and kinetics, J. Hazard. Mater. 434 (2022), 128910, https://doi.org/10.1016/j.jhazmat.2022.128910.

[22] S. Chen, W. Zhang, J. Li, M. Yuan, J. Zhang, F. Xu, H. Xu, X. Zheng, L. Wang, Ecotoxicological effects of sulfonamides and fluoroquinolones and their removal by a green alga (*Chlorella vulgaris*) and a cyanobacterium (*Chrysosporum ovalisporum*), Environ. Pollut. 263 (2020), 114554, https://doi.org/10.1016/j.envpol.2020.114554.

[23] M.E. Conrad, E.L. Brodie, C.W. Radtke, M. Bill, M.E. Delwiche, M.H. Lee, D. L. Swift, F.S. Colwell, Field evidence for co-metabolism of trichloroethene stimulated by addition of electron donor to groundwater, Environ. Sci. Technol. 44 (12) (2010) 4697–4704, https://doi.org/10.1021/es903535j.

[24] Q. Xiong, Y.-S. Liu, L.-X. Hu, Z.-Q. Shi, W.-W. Cai, L.-Y. He, G.-G. Ying, Co-metabolism of sulfamethoxazole by a freshwater microalga *Chlorella pyrenoidosa*, Water Res. 175 (2020), 115656, https://doi.org/10.1016/j.watres.2020.115656.

[25] H.N.P. Vo, H.H. Ngo, W. Guo, Y. Liu, S. Woong Chang, D.D. Nguyen, X. Zhang, H. Liang, S. Xue. Selective carbon sources and salinities enhance enzymes and extracellular polymeric substances extrusion of *Chlorella* sp. for potential co-metabolism. Bioresour. Technol. 303. (2020). 122877. https://doi.org/10.1016/j.biortech.2020.122877.

[26] C. Kiki, A. Rashid, Y. Zhang, X. Li, T.-Y. Chen, A.B. Eloise Adéoye, P.O. Peter, Q. Sun. Microalgal mediated antibiotic co-metabolism: Kinetics, transformation products and pathways. Chemosphere. 292. (2022). 133438. https://doi.org/10.1016/j.chemosphere.2021.133438.

[27] F. Gao, L. Yang, A.-J. Chen, W.-H. Zhou, D.-Z. Chen, J.-M. Chen, Promoting effect of plant hormone gibberellin on co-metabolism of sulfamethoxazole by microalgae *Chlorella pyrenoidosa*, Bioresour. Technol. 351 (2022), 126900, https://doi.org/10.1016/j.biortech.2022.126900.

[28] N.H. Tran, T. Urase, H.H. Ngo, J. Hu, S.L. Ong, Insight into metabolic and cometabolic activities of autotrophic and heterotrophic microorganisms in the biodegradation of emerging trace organic contaminants, Bioresour. Technol. 146 (2013) 721–731, https://doi.org/10.1016/j.biortech.2013.07.083.

[29] Y.-Y. Cheng, W.-J. Wang, S.-T. Ding, M.-X. Zhang, A.-G. Tang, L. Zhang, D.-B. Li, B.-B. Li, G.-Z. Deng, C. Wu, Pyruvate accelerates palladium reduction by regulating catabolism and the electron transfer pathway in *Shewanella oneidensis*, Appl. Environ. Microbiol. 87 (8) (2021) e02716–e2720, https://doi.org/10.1128/AEM.02716-20.

[30] C. Liang, L. Zhang, N.B. Nord, P.N. Carvalho, K. Bester, Dose-dependent effects of acetate on the biodegradation of pharmaceuticals in moving bed biofilm reactors, Water Res. 159 (2019) 302–312, https://doi.org/10.1016/j.watres.2019.04.026.

[31] X. Wang, M.-M. Zhang, Z. Sun, S.-F. Liu, Z.-H. Qin, J.-H. Mou, Z.-G. Zhou, C.S. K. Lin, Sustainable lipid and lutein production from *Chlorella* mixotrophic fermentation by food waste hydrolysate, J. Hazard. Mater. 400 (2020), 123258, https://doi.org/10.1016/j.jhazmat.2020.123258.

[32] H. El-taliawy, M.E. Casas, K. Bester, Removal of ozonation products of pharmaceuticals in laboratory Moving Bed Biofilm Reactors (MBBRs), J. Hazard. Mater. 347 (2018) 288–298, https://doi.org/10.1016/j.jhazmat.2018.01.002.

[33] X. Wang, S.-F. Liu, Z.-H. Qin, S. Balamurugan, H.-Y. Li, C.S.K. Lin, Sustainable and stepwise waste-based utilisation strategy for the production of biomass and biofuels by engineered microalgae, Environ. Pollut. 265 (2020), 114854, https://doi.org/10.1016/j.envpol.2020.114854.

[34] L. Zhang, C. Zhang, J. Liu, N. Yang, A strategy for stimulating astaxanthin and lipid production in *Haematococcus pluvialis* by exogenous glycerol application under low light, Algal Res. 46 (2020), 101779, https://doi.org/10.1016/j.algal.2019.101779.

[35] M. Zhang, A.D. Steinman, Q. Xue, Y. Zhao, Y. Xu, L. Xie, Effects of erythromycin and sulfamethoxazole on Microcystis aeruginosa: Cytotoxic endpoints, production and release of microcystin-LR, J. Hazard. Mater. 399 (2020), 123021, https://doi.org/10.1016/j.jhazmat.2020.123021.

[36] L. Zhang, R. Guo, H. Li, Q. Du, J. Lu, Y. Huang, Z. Yan, J. Chen, Mechanism analysis for the process-dependent driven mode of NaHCO3 in algal antibiotic removal: efficiency, degradation pathway and metabolic response, J. Hazard. Mater. 394 (2020), 122531, https://doi.org/10.1016/j.jhazmat.2020.122531.

[37] G. Chen, B. Wang, D. Han, M. Sommerfeld, Y. Lu, F. Chen, Q. Hu, Molecular mechanisms of the coordination between astaxanthin and fatty acid biosynthesis in *Haematococcus pluvialis* (Chlorophyceae), Plant J. 81 (1) (2015) 95–107, https://doi.org/10.1111/tpj.12713.

[38] J.-Q. Xiong, S. Ru, Q. Zhang, M. Jang, M.B. Kurade, S.-H. Kim, B.-H. Jeon, Insights into the effect of cerium oxide nanoparticle on microalgal degradation of sulfonamides, Bioresour. Technol. 309 (2020), 123452, https://doi.org/10.1016/j.biortech.2020.123452.

[39] I.M. Møller, PLANT MITOCHONDRIA AND OXIDATIVE STRESS: Electron transport, NADPH turnover, and metabolism of reactive oxygen species, Annu. Rev. Plant Physiol. Plant Mol. Biol. 52 (1) (2001) 561–591, https://doi.org/10.1146/annurev.arplant.52.1.561.

[40] X. Li, C. Yang, G. Zeng, S. Wu, Y. Lin, Q. Zhou, W. Lou, C. Du, L. Nie, Y. Zhong, Nutrient removal from swine wastewater with growing microalgae at various zinc concentrations, Algal Res. 46 (2020), 101804, https://doi.org/10.1016/j.algal.2020.101804.

[41] S. Wang, K. Poon, Z. Cai, Removal and metabolism of triclosan by three different microalgal species in aquatic environment, J. Hazard. Mater. 342 (2018) 643–650, https://doi.org/10.1016/j.jhazmat.2017.09.004.

[42] S. Hena, L. Gutierrez, J.-P. Croué, Removal of pharmaceutical and personal care products (PPCPs) from wastewater using microalgae: A review, J. Hazard. Mater. 403 (2021), 124041, https://doi.org/10.1016/j.jhazmat.2020.124041.

[43] D.L. Sutherland, P.J. Ralph, Microalgal bioremediation of emerging contaminants - Opportunities and challenges, Water Res. 164 (2019), 114921, https://doi.org/10.1016/j.watres.2019.114921.

[44] Z. Lu, Y. Xu, L. Peng, C. Liang, Y. Liu, B.-J. Ni, A two-stage degradation coupling photocatalysis to microalgae enhances the mineralization of enrofloxacin, Chemosphere 293 (2022), 133523, https://doi.org/10.1016/j.chemosphere.2022.133523.
[45] J. Zhang, A. Xia, D. Yao, X. Guo, S.S. Lam, Y. Huang, X. Zhu, X. Zhu, Q. Liao, Removal of oxytetracycline and ofloxacin in wastewater by microalgae-bacteria symbiosis for bioenergy production, Bioresour. Technol. 363 (2022), 127891, https://doi.org/10.1016/j.biortech.2022.127891.
[46] R. Fu, X. Li, Y. Zhao, Q. Pu, Y. Li, W. Gu, Efficient and synergistic degradation of fluoroquinolones by bacteria and microalgae: Design of environmentally friendly substitutes, risk regulation and mechanism analysis, J. Hazard. Mater. 437 (2022), 129384, https://doi.org/10.1016/j.jhazmat.2022.129384.
[47] J.-Q. Xiong, M.B. Kurade, B.-H. Jeon, Biodegradation of levofloxacin by an acclimated freshwater microalga, *Chlorella vulgaris*, Chem. Eng. J. 313 (2017) 1251–1257, https://doi.org/10.1016/j.cej.2016.11.017.
[48] Y. Chu, C. Zhang, R. Wang, X. Chen, N. Ren, S.-H. Ho, Biotransformation of sulfamethoxazole by microalgae: Removal efficiency, pathways, and mechanisms, Water Res. 221 (2022), 118834, https://doi.org/10.1016/j.watres.2022.118834.
[49] E.M. Isin, F.P. Guengerich, Complex reactions catalyzed by cytochrome P450 enzymes, Biochim. Biophys. Acta Gen. Subj. 1770 (3) (2007) 314–329, https://doi.org/10.1016/j.bbagen.2006.07.003.
[50] K. Sargsyan, C. Grauffel, C. Lim, How molecular size impacts RMSD applications in molecular dynamics simulations, J. Chem. Theory Comput. 13 (4) (2017) 1518–1524, https://doi.org/10.1021/acs.jctc.7b00028.
[51] M.Y. Lobanov, N.S. Bogatyreva, O.V. Galzitskaia, Radius of gyration is indicator of compactness of protein structure, Mol. Biol. 42 (4) (2008) 701–706, https://doi.org/10.1134/S0026893308040195.
[52] W. Lin, Y. Yan, S. Ping, P. Li, D. Li, J. Hu, W. Liu, X. Wen, Y. Ren, Metformin-induced epigenetic toxicity in zebrafish: Experimental and molecular dynamics simulation studies, Environ. Sci. Technol. 55 (3) (2021) 1672–1681, https://doi.org/10.1021/acs.est.0c06052.
[53] H. Cao, Z. Zhou, L. Wang, G. Liu, Y. Sun, Y. Wang, T. Wang, Y. Liang, Screening of potential PFOS alternatives to decrease liver bioaccumulation: Experimental and computational approaches, Environ. Sci. Technol. 53 (5) (2019) 2811–2819, https://doi.org/10.1021/acs.est.8b05564.